Gamma radiolytic synthesis of poly(2, 3-Epoxy-propylmethacrylate)-stabilized-gold nanoparticles: an efficient catalyst for *p*-nitrophenol reduction

Nilanjal Misra[1]*, Virendra Kumar[1,2]*, Swarnima Rawat[1], Narender Kumar Goel[1], Shubhangi A. Shelkar[1], Lalit Varshney[1,2]

[1]*Radiation Technology Development Division, Bhabha Atomic Research Centre, Trombay, Mumbai 400085, India*
[2]*Homi Bhabha National Institute, Anushaktinagar, Mumbai 400094, India*

*Corresponding authors

Abstract

A facile, green radiolytic route is described for the synthesis of poly (2,3-Epoxypropylmethacrylate) (PEPMA) stabilized Gold nanoparticles (PEPMA-Au-NPs) via gamma radiolytic reduction of an aqueous solution of $HAuCl_4$ precursor ions containing EPMA as a stabilizing/capping agent. The effect of different experimental parameters, such as precursor ions and stabilizing agent concentration, gamma radiation dose and solvent polarity on the properties of Au-NPs were studied. PEPMA-Au-NPs system was characterized by UV-visible spectroscopy, TEM and particle size analysis techniques. PEPMA-Au-NPs showed characteristic Localized Surface Plasmon Resonance (LSPR) band at ~530nm. TEM analysis confirmed the formation of spherical particles with an average size of 7.6nm±3.1nm. PEPMA-Au NPs prepared under optimized conditions were employed as an efficient catalytic system to carry out the reduction of *p*-nitrophenol (PNP) to *p*-aminophenol (PAP). The reaction was observed to follow pseudo first order kinetics and demonstrated good efficiency in carrying out the catalytic reduction reaction under optimized conditions. Copyright © 2018 VBRI Press.

Keywords: Gamma radiation, Gold nanoparticles, 2,3-Epoxypropylmethacrylate, Catalysis, *p*-nitrophenol.

Introduction

Metal nanoparticles find applications in a wide array of fields, including catalysis [1], antibacterial agents [2], drug delivery systems [3] chemical and bio sensors [4,5]. The intense Localized Surface Plasmon Resonance (LSPR) absorption in the visible region of noble metal nanoparticles [6], such as those of Au and Ag, make them potential candidates for optical biosensor applications [7,8]. Moreover, high specific surface area, leading to high reactivity, make these noble metal nanoparticles extremely efficient catalytic materials to carry out reactions that are otherwise difficult to initiate [9-11].

Although literature provides numerous chemical methods for fabrication of noble metal nanoparticles, most of these methods suffer from limitations in terms of use of toxic chemical reducing agents, harsh reaction conditions, poor size distribution, control over reaction parameters, etc. Therefore, in recent years, radiolytic reduction route for generation of metal nanoparticles has gained popularity as an attractive alternative to these chemical reduction methods. [60]Co gamma radiation based synthetic route involves not only more convenient and simpler control parameters for engineering nanoparticles of desired morphology but is also a clean, room temperature technique that does not involve use of any external reducing agents [7,8,12-15]. The choice of capping agent/ stabilizer during synthesis of metal nanoparticles influences the overall stability and morphology of the particles generated, which in turn decides the long term utility of the system as a facile catalytic or sensor system [7,8,16]. The aggregation of nanoparticles, for instance, will greatly diminish their specific surface area and consequently lower the catalytic efficiency. To enhance the catalytic efficiency and overcome limitations, such as high cost and limited supply of nanoparticles for practical applications, it is therefore important to use capping agents that provide optimum stability to the nanoparticle systems and make their use economically viable [17-19].

Gold, silver and palladium noble metal nanoparticles are known to catalyze a range of organic and inorganic reactions. One of the important reactions, catalyzed by such catalytic systems, is the reduction of *p*-nitrophenol (PNP) to *p*-aminophenol (PAP) in presence of $NaBH_4$ as the reducing agent. This reaction has high industrial relevance since PAP is a building block compound and is an important intermediate produced in the syntheses of various chemicals including dyes, pharmaceuticals (e.g., paracetamol), and anticorrosive lubricants [20-22]. PAP is also used in the cosmetics and personal care industry as formulations for permanent hair dyes, colors and tints. Recently, Wu *et al.* have reported the green synthesis of gold nanoparticles using aspartame as a

reducing agent and studied their catalytic activity for *p*-nitrophenol reduction [23]. Lin *et al.* synthesized Al_2O_3 supported Au nanoparticles and investigated their catalytic properties [24]. Biogenic gold and silver nanoparticles have been reported to possess good catalytic properties [25]. Silver nanoparticles synthesized inside porous anion exchange membranes have also been demonstrated to possess excellent catalytic properties [26].

The present work highlights, to the best of our knowledge, the first reported application of poly (2,3-Epoxypropylmethacrylate) (PEPMA) as an effective stabilizer/ capping agent in the gamma radiation induced synthesis of size controlled, uniformly dispersed, spherical Gold nanoparticles (PEPMA-Au NPs) with long term stability. The catalytic efficiency of the PEPMA-Au NPs system was tested by taking the catalytic reduction of *p*-nitrophenol (PNP) to *p*-aminophenol (PAP) in presence of $NaBH_4$, as a model reaction.

Experimental

Reagents

Hydrogen tetrachloroaurate trihydrate (purity = 99.99%, MV laboratories Inc.), 2,3-epoxypropylmethacrylate (EPMA, purity = 97%, Sigma Aldrich), 2-propanol (Analytical reagent grade, Polypharm, India), *p*-nitrophenol (PNP, purity = 99.5%, Sigma Aldrich), $NaBH_4$ (purity = 98.5%, Sigma Aldrich) and N_2 gas (purity=99.998%, Inox air products, India) were used as received. All aqueous solutions were prepared in ultra-pure water with resistivity = $18 M\Omega.cm$ produced using water purification system 'Ultraclear TWF UV' (SG Wasseraufbereitung & Regenerierstation GmbH, Germany).

Characterization techniques

An Evolution 300 (Thermoelectron, UK) UV-visible spectrophotometer, with wavelength region of 250-1000 nm and resolution of 1 nm was used to record the UV-visible absorption spectra of the PEPMA-Au NPs solutions.

Transmission Electron Microscopy (TEM) analysis was carried out with an Energy Filtering Transmission Electron Microscope (EF-TEM, LIBRA 120, Carl Zeiss) at an accelerating voltage of 120 kV in order to determine the shape and size of the Au nanoparticles. For the TEM analysis, PEPMA-Au-NPs were deposited on a carbon coated copper grid by placing dilute NPs solution on it and drying in a Laminar flow hood. An *Image J1.49* software was employed for the particle size distribution analysis of the TEM images.

The hydrodynamic diameter of Au nanoparticles was measured using Particle Size Analyzer (VASCO 3, Cordouan, France). The measurement was replicated three times per sample to ensure reproducibility of obtained results.

Radiolytic synthesis of PEPMA-Au NPs

A ^{60}Co gamma chamber (GC 5000, BRIT, India) having radiation dose rate of 2.0 kGy hr^{-1} was used for gamma irradiations of samples. The dose rate was determined using Fricke dosimetry [27]. A reaction mixture comprising of 1.0×10^{-4} $mol.dm^{-3}$ Au^{3+}, 0.1% (v/v) EPMA and 40% (v/v) 2-propanol in aqueous medium, was subjected to N_2 purging followed by irradiation to a pre determined gamma radiation dose. Appearance of a pinkish-violet coloration signaled the formation of PEPMA-Au NPs, further confirmed by the characteristic Localized Surface Plasmon Resonance (LSPR) absorption band of Au NPs at ~530nm.

Catalytic reduction of p-nitrophenol

Aqueous solutions of *p*-nitrophenol and $NaBH_4$ were mixed to maintain a final molar ratio of 1:100 (*p*-nitrophenol:$NaBH_4$). An optimized concentration of radiolytically synthesized PEPMA-Au-NPs solution was added as a catalyst to the reaction mixture. The catalytic reduction of PNP to PAP was monitored via UV-visible spectrophotometry in the spectral range of 280-450nm.

Results and discussion

Radiolytic synthesis of PEPMA-Au NPs

Gamma radiolytic synthesis of PEPMA-Au NPs was carried out by irradiating an aqueous solution containing Au^{3+}, EPMA and 2-propanol, purged with N_2 gas. Radiolysis of water yields reactive transient species, *viz.,* e_{aq}^-, $H^.$, $^.OH$, etc. 2-propanol present in the reaction medium reacts with radicals $H^.$ and $^.OH$ to generate 2-propyl radical, a mild reducing agent capable of reducing Au^{3+} to metal in zero valent state (Au^0). The overall reduction in this reaction medium is therefore carried out by the two reducing species, *viz.* e_{aq}^- and $(CH_3)_2C^.-OH$. Subsequent to the initial reduction step, coalescence of the Au^0 atoms results in the formation of Au nanoclusters. Simultaneously, radiation induced polymerization of EPMA also takes place in the reaction medium resulting in the formation of PEPMA, which acts as a capping agent, and regulates the size and morphology of the metal nanoparticles. The detailed mechanism of radiolytic synthesis of metal nanoparticles has been discussed in our earlier work [8].

Characterization of PEPMA-Au NPs

Fig. 1 presents the UV-visible spectra of aqueous solution of PEPMA-Au NPs system prepared at varying gamma radiation doses under optimized reaction conditions, showing strong LSPR absorption band at ~530nm, typical of spherical Au nanoparticles. The shape and size of the PEPMA-Au NPs were further determined by TEM analysis. TEM micrographs revealed the freshly prepared PEPMA-Au NPs to be mainly spherical in nature **[Fig. 2a],** with particle size distribution analysis calculating the average particle size to be 7.6nm±3.1nm

[Fig. 2b]. The hydrodynamic size of the PEPMA-Au NPs was also determined using a particle size analyzer and found in good agreement with the TEM analysis results.
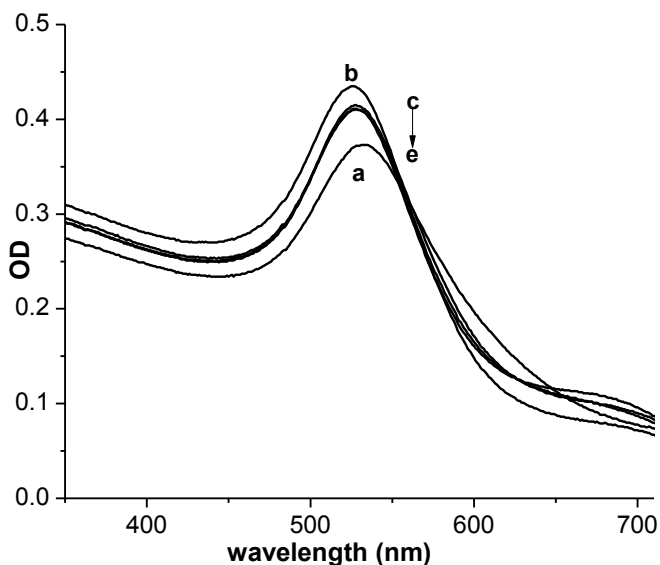

Fig. 1. UV-visible spectra of PEPMA-Au NPs at gamma radiation doses (a) 0.5 (b) 1.0 (c) 1.5 (d) 2.0 and (e) 3.0 kGy ([2-propanol]=40% (v/v), [Au^{3+}]=1.0×10^{-4} mol dm^{-3}, [EPMA]=0.1% (v/v)).

Effect of radiation dose on formation of PEPMA-Au NPs

Radiation dose is one of the vital parameters governing the size, shape and morphology of noble metal nanoparticles synthesized via radiolytic route. As evident from **Fig.1,** PEPMA-Au NPs prepared at 0.5kGy dose ([Au^{3+}] =1.0×10^{-4} mol.dm^{-3}, [EPMA]=0.1% (v/v)) yielded a single broad peak with a λ_{max}~530nm, which corresponds to the LSPR band of spherical PEPMA-Au NPs. Increase in the radiation dose (keeping all other parameters constant) to 1.0kGy increased the intensity of the LSPR band. This can be attributed to the increased reduction of Au^{3+} ions at higher radiation doses resulting in the generation of higher number of Au nanoparticle species.

A slight blue shift in the LSPR band was also observed which was probably due to a decrease in the average particle size of the nanoparticles formed at higher radiation doses [28,29]. However, further increase in the radiation dose resulted in a slight decrease in intensity of the LSPR band coupled with the appearance of a second broad, low intensity peak at around ~680nm. The second peak implies formation of a small fraction of larger aggregates in addition to the predominantly small sized particles. Hence, for all further experiments radiation dose for reduction of 1.0×10^{-4} mol dm^{-3} Au^{3+} ion solution was optimized at 1.0kGy.

Effect of solvent composition on formation of PEPMA-Au NPs

Fig. 3A presents the UV-Visible spectra of PEPMA-Au NPs solution synthesized at 1.0kGy dose under varying
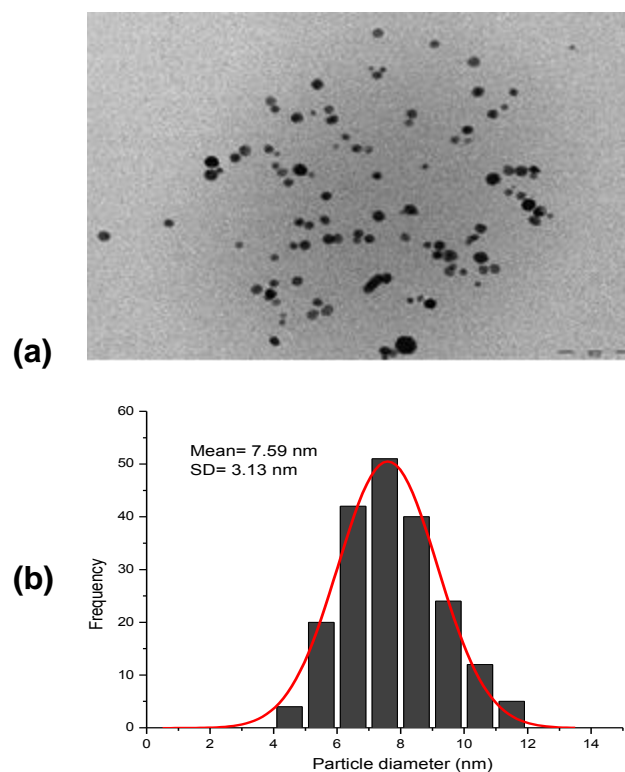

Fig. 2. (a) TEM image of PEPMA-Au NPs and (b) Particle size distribution data for PEPMA-Au NPs.

solvent ratios ([Au^{3+}] =1.0×10^{-4} mol.dm^{-3}, [EPMA]=0.1% (v/v)). The composition of the solvent used plays pivotal role in regulating the process of Au nanoparticles formation as well as in determining the solubility of the capping agent in the reaction mixture. Since EPMA has limited solubility in water, a minimum 2-propanol:water ratio of 3:7 was used to ensure its complete dissolution.

A solvent mixture with 2-propanol:water ratio of 2:3 yielded a single peak at ~530nm, whereas, increase in 2-propanol:water ratio to 3:2 led to a broadening of the LSPR band and appearance of a second, broad peak at around ~650nm. Further increase in 2-propanol:water ratio up to 9:1 led to near flattening of the LSPR band. Therefore, the 2-propanol:water ratio was optimized at 2:3 to ensure the formation of uniformly dispersed, spherical nanoparticles. This observation can be explained on the basis of the weaker reducing power of (CH$_3$)$_2$C·-OH (E^0=-1.8 V$_{NHE}$) compared to e$_{aq}^-$ (E^0=-2.9 V$_{NHE}$). (CH$_3$)$_2$C·-OH radical reduces only Au^{3+} ions that are adsorbed onto the surface of Au clusters, since they have higher reduction potentials as compared to metal ions in the free state [30,31]. On the other hand, Au^{3+} ions in free state are reduced by the stronger reducing agent, i.e., e$_{aq}^-$, and act as the seeds on which subsequent nucleation and growth of the nanoclusters occurs. With increase in 2-propanol concentration in the reaction mixture, the ratio of concentration of CH$_3$)$_2$C·-OH to e$_{aq}^-$ will increase, leading to formation of larger nanoparticles with broad size distribution, which is evident from the broad spectral signature obtained for PEPMA-Au NPs prepared at higher 2-propanol:water ratios.

Effect of EPMA concentration on formation of PEPMA-Au NPs

Fig. 3B shows the absorption spectra for PEPMA-Au NPs solution synthesized at radiation dose of 1.0kGy ($[Au^{3+}]$ =1.0×10^{-4} mol.dm^{-3}, 2-propanol:water =2:3) under varying concentrations of EPMA. No significant change in the spectral behavior of the LSPR band of PEPMA–Au NPs was observed when the concentration of EPMA was varied from 0.1% to 0.4% (v/v). However, at higher EPMA concentrations of 0.5% and 1.0%, the overall intensity of the UV-visible spectra was found to increase drastically. This may be attributed to the additive contribution of absorbance due to higher concentration of PEPMA formed during irradiation, leading to the increase in OD of the overall absorption spectra of PEPMA-Au NPs system, predominantly in the lower wavelength region. However, there was no significant effect of PEPMA on the position of LSPR band of PEPMA-Au NPs system, thereby, implying no effect on the average size of the PEPMA–Au-NPs.
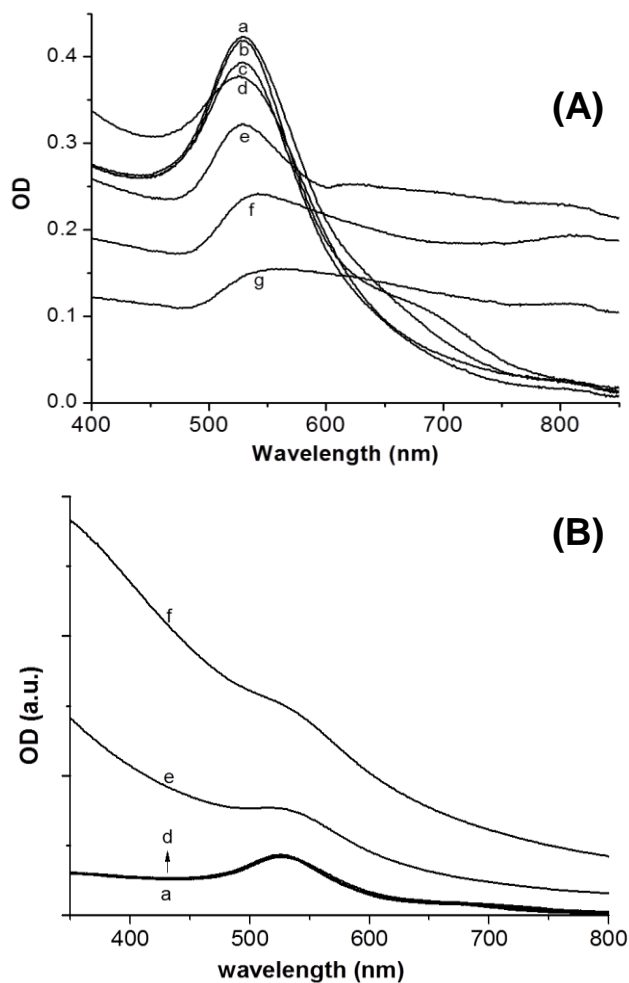

Fig. 3. (A) UV-visible spectra of PEPMA-Au NPS in solvent systems with varying 2-propanol:water ratio (a) 3:7 (b) 2:3 (c) 1:1 (d) 3:2 (e) 7:3 (f) 4:1 and (g) 9:1. ($[Au^{3+}]$=1.0×10^{-4} mol.dm^{-3}, [EPMA]=0.1% (v/v), Dose= 1.0kGy) **(B)** UV-visible spectra of PEPMA-Au NPs containing varying concentration % (v/v) of EPMA (a) 0.1 (b) 0.2 (c) 0.3 (d) 0.4 (e) 0.5 and (f) 1.0 % (w/v) ($[Au^{3+}]$= 1×10^{-4} mol dm^{-3}, 2-propanol:water=2:3, Dose= 1.0kGy)

Effect of Au^{3+} concentration on formation of PEPMA-Au NPs

Fig. 4A presents the UV-visible spectra of PEPMA-Au NPs prepared at different precursor ion concentrations (total dose=1.0 kGy, [EPMA]=0.1% (v/v), 2-propanol: water=2:3). Increase in Au^{3+} concentration from 1.0×10^{-4} mol.dm^{-3} to 4.0×10^{-4} mol.dm^{-3} was accompanied by a steady increase in the intensity of LSPR band, indicating increase in yield of PEPMA-Au NPs. However, at 5.0×10^{-4} mol.dm^{-3}, intensity of the LSPR band of PEPMA-Au NPs was again found to decrease with appearance of an additional peak at ~315nm, which corresponds to unreduced Au^{3+} ions. This indicates that the reduction of 5.0×10^{-4} mol.dm^{-3} Au^{3} ions was incomplete under the given reaction conditions. Moreover, at higher precursor concentrations, an additional broad hump started appearing above ~700nm, which may be attributed to the formation of large Au aggregates. It is known that the competition between reduction of free metal ions and the ions adsorbed on surface of the clusters is controlled by the rate of formation of reducing agent. At high Au^{3+} ion concentrations, the number of gamma radiolytically generated reducing species, at any given instant, becomes insufficient to reduce all the Au^{3+} ions to Au atoms in the zerovalent state [30,32]. Consequently, the rate of adsorption of Au^{3+} ions, which are abundantly available in the solution, onto the Au clusters becomes dominant, resulting in the preferential reduction of the surface adsorbed Au^{3+} ions and subsequent formation of large Au aggregates.

Storage stability of PEPMA-Au NPs

The PEPMA-Au NPs were found to possess good stability when stored at 4^{0}C. UV-visible spectra of the PEPMA-Au NPs recorded at intervals of 30 days showed negligible change. The LSPR peak of PEPMA-Au NPs system, prepared at a radiation dose of 1.0kGy ($[Au^{3+}]$ =1.0×10^{-4} mol.dm^{-3}, [EPMA]= 0.1% (v/v), 2-propanol:water=2:3) was observed to undergo only a minute red shift after a period of six months, thereby highlighting the excellent capping property of PEPMA as a stabilizer for synthesis of Au NPs.

PEPMA-Au NPs catalyzed reduction of p-nitrophenol to p-aminophenol

The catalytic activity of PEPMA-Au NPs was investigated by monitoring the reduction of *p*-nitrophenolate to *p*-aminophenolate in presence of NaBH$_4$. Briefly, 0.5 ml each of an aqueous solution of PNP (5.0×10^{-3} mol.dm^{-3} stock solution) and NaBH$_4$ (5.0x10^{-1} mol.dm^{-3} stock solution) was diluted to 9 ml using deionized water. To this solution was added 1.0ml of 1.0×10^{-4} mol dm^{-3} solution of PEPMA-Au NPs (final catalyst concentration = 1.0×10^{-5} mol.dm^{-3} and PNP:NaBH$_4$ = 1:100). The reaction was monitored spectrophotometrically within a wavelength range of 280-450 nm.
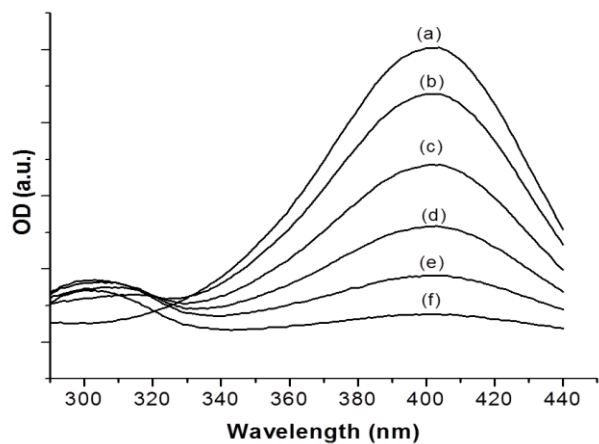
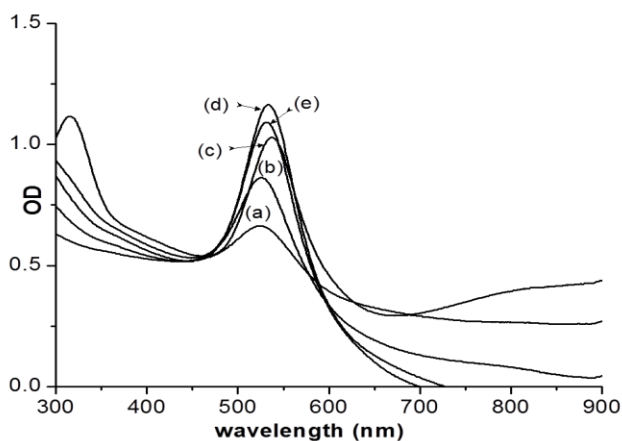**Fig. 4. (A)** UV-visible spectra of PEPMA-Au NPs solution prepared with varying concentration of Au^{3+} ions (a) 1.0×10^{-4} mol dm^{-3} (b) 2.0×10^{-4} mol dm^{-3} (c) 3.0×10^{-4} mol dm^{-3} (d) 4.0×10^{-4} mol dm^{-3} and (e) 5.0×10^{-4} mol dm^{-3} (Dose=1.0 kGy, [EPMA]=0.1% (v/v), 2:3 (2-propanol:water) medium) **(B)** UV-visible spectra of PNP-NaBH$_4$ reaction system in presence of PEPMA-Au NPs catalyst after (a) 0 (b) 5 (c) 10 (d) 15 (e) 20 and (f) 25 minutes ([PEPMA-Au NPs] = 1.0×10^{-5} mol.dm^{-3}, PNP:NaBH$_4$ molar ratio=1:100)

The UV-visible spectra of PNP solution exhibits a strong absorption peak at ~317 nm which is instantaneously red-shifted to ~400 nm when treated with an aqueous solution of NaBH$_4$ **(Fig. 4B)** [33-35]. The absorption at 400 nm arises due to the formation of p-nitrophenolate ions in presence of NaBH$_4$ owing to an increase in solution alkalinity. The intense yellow colour of *p*-nitrophenolate ions (~400 nm) remains unchanged in the absence of any catalysts [36]. However, addition of PEPMA-Au NPs solution to the *p*-nitrophenolate solution results in a gradual decrease in the peak intensity with time. The probable mechanism of the catalytic reaction **(Fig. 5),** as suggested by Seodi et al. [10], involves the PEPMA-Au NPs catalyst acting as a hydrogen carrier between NaBH$_4$ and PNP. NaBH$_4$, in presence of H$_2$O, generates H$_2$ (Eqn. 1) which is responsible for the reduction of PNP to PAP. The inherent adsorption-desorption behavior of H$_2$ on the surface of Au NPs facilitates the transportation of the H$_2$ generated to the vicinity of the substrate site of PNP, which subsequently carries out the reduction.
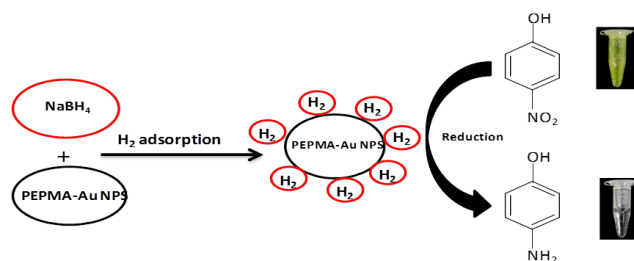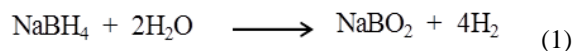

Fig. 5. PEPMA-Au NPs Catalyzed reduction of *p*-nitrophenol to *p*-aminophenol in presence of NaBH$_4$.

$$NaBH_4 + 2H_2O \longrightarrow NaBO_2 + 4H_2 \quad (1)$$

The catalytic reaction was monitored by varying the concentrations of the PEPMA-Au NPs catalyst. Since NaBH$_4$ was used in excess (molar ratio of 1:100), its concentration could be assumed as constant and the overall reaction reduced to a pseudo first order type of reaction with respect to PNP. By fitting into the equation for pseudo first order law (Eqn. 2), the apparent rate constants were calculated**.**

$$\ln \frac{c_t}{c_0} = -kt \quad (2)$$

where, C_t= Concentration of PNP at time 't', C_0= Initial concentration of PNP and k=Apparent rate constant.
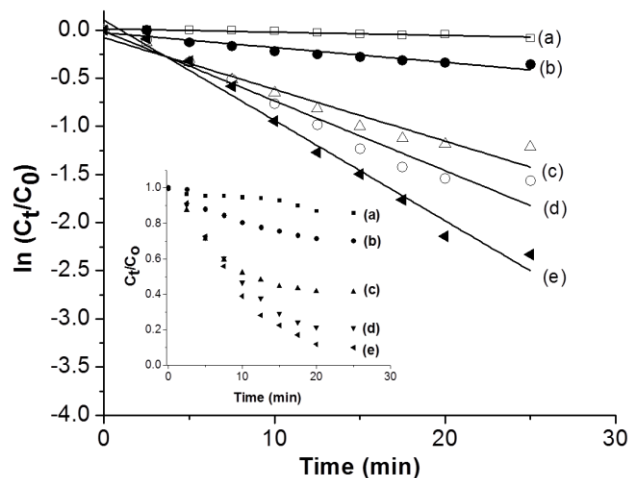

Fig. 6. Plot of $\ln(C_t/C_0)$ *vs* time as a function of PEPMA-Au NPs concentrations: (a)1.0 μM (b) 2.5 μM (c) 5.0 μM (d) 7.5 μM and (e) 10.0 μM) ([PNP]= 50 μM). (Inset: C_t/C_0 *vs* time plots as a function of PEPMA-Au NPs concentrations: (a)1.0 μM (b) 2.5 μM (c) 5.0 μM (d) 7.5 μM and (e) 10.0 μM)

Fig. 6 inset presents the decrease in the relative concentration of substrate PNP (C_t/C_0) with time at different concentrations of the PEPMA-Au NPs catalytic system. It can be seen that the rate of reduction of PNP to PAP in presence of NaBH$_4$ increased with the increase in catalyst concentration. This is in concurrence with the results reported by Nalawade *et al.* [37]. In order to calculate the apparent rate constants at different catalyst

concentrations, $\ln(C_t/C_0)$ was plotted against reaction time **(Fig. 6)**. The linear plots obtained at different catalyst concentrations clearly indicated that the reaction follows pseudo first order kinetics. The apparent rate constants, calculated from the slopes of the plots obtained for varying catalyst concentrations, are presented in **Table 1**. Another important parameter frequently used to quantify the efficacy of any catalyst is the Turnover Frequency (TOF), which is defined as the number of moles of product formed per mole of catalyst concentration per unit time. The TOF for 10 μM (i.e., 1.90×10^{-3} mg.mL^{-1}) catalyst concentration was determined to be 10.8 h^{-1}, which is comparable to the catalytic efficiency reported earlier in the literature for similar catalytic systems **(Table 2)** [38-41].

Table 1. Rate constant determination under varying PEPMA-Au NPs catalyst concentrations.

Final amount of catalyst (mg.mL^{-1})	PNP (μM)	Apparent rate constant k (s^{-1})
1.90×10^{-4} (1.0 μM)	50	5.00×10^{-5}
4.75×10^{-4} (2.5 μM)	50	2.50×10^{-4}
9.50×10^{-4} (5.0 μM)	50	8.83×10^{-4}
1.43×10^{-3} (7.5 μM)	50	1.20×10^{-3}
1.90×10^{-3} (10.0 μM)	50	1.73×10^{-3}

Table 2. Comparison of catalytic systems prepared by different processes for reduction of *p*-nitrophenol to *p*-aminophenol.

Catalyst	Method of preparation	[*p*-nitrophenol] (mM)	[NaBH₄] (mM)	Rate Constant (s^{-1})	Ref.
PEPMA-Au NPs Au/graphene Au/Tween/GO Ag NPs Ag NPs	**Gamma radiolytic synthesis** Self assembly under hydrothermal condition Chemical reduction Sol-gel method Wet chemical reduction	0.05 0.10 7.0 5.0 0.1	5.00 100.00 0.16 100.00 100.00	1.73×10^{-3} 3.16×10^{-3} 4.16×10^{-3} 1.83×10^{-3} 3.18×10^{-3}	This work [38] [39] [40] [41]

Conclusion

The work highlights the first reported use of PEPMA as an efficient stabilizer/capping agent in the gamma radiolytic synthesis of Au nanoparticles using gamma radiation. Radiation dose and solvent polarity were found to influence the process of nanoparticles formation. These parameters were accordingly optimized at 1.0kGy and 2:3 (2-propanol:water) solvent mixture to generate spherical

PEPMA-Au NPs with uniform size distribution. The PEPMA-Au NPs were observed to possess high storage stability of more than six months when stored at 4⁰C. Radiation synthesized PEPMA-Au NPs system was employed as an efficient catalytic system to carry out the reduction of *p*-nitrophenol (PNP) to *p*-aminophenol (PAP) in presence of NaBH₄. The reaction was observed to follow pseudo first order kinetics and demonstrated good efficiency in carrying out the industrially relevant reaction under optimized conditions.

References

1. Sharma, N.; Ojha, H.; Bharadwaj, A.; Pathak, D.P.; Sharma, R.K. *RSC Adv.* **2015**, *5*, 53381.
2. Rawashdeh, R.; Haik, Y. Antibacterial mechanisms of metallic nanoparticles: a review. In Dynamic biochemistry, process biotechnology and molecular biology, **2009**, 3, 12.
3. Ahmad, M.Z.; Akhter, S.; Jain, G.K.; Rahman, M.; Pathan, S.A.; Ahmad, F.J.; Khar, R.K. *Expert Opin. Drug Delivery,* **2010**, *7*, 927.
4. Shen, G.; Chen, P.C.; Ryu, K.; Zhou, C. *J. Mater. Chem.* **2008**, *19*, 828.
5. Holzinger, M.; Goff, A.L.; Cosnier, S. *Front. Chem.* **2014**, *2*, 63.
6. Creighton, J.A.; Eadont, D.G. *J. Chem. Soc., Faraday Trans.* **1991**, *87*, 3881.
7. Misra, N.; Kumar, V.; Borde, L.; Varshney, L. *Sens. Actuators, B,* **2013**, *178*, 371.
8. Misra, N.; Biswal, J.; Gupta, A.; Sainis, J.K.; Sabharwal, S. *Radiat. Phys. Chem.* **2012**, *81*, 195.
9. Fenger, R.; Fertitta., E; Kirmse, H.; Thunemann, A.F.; Rademann, K. *Phys. Chem. Chem. Phys.* **2012**, *14*, 9343.
10. Seoudi, R.; Said, D.A. *World J. Nano Sci. Eng.* **2011**, *1*, 51.
11. Hvolbæk, B.; Janssens, T.V.W.; Clausen, B.S.; Falsig, H.; Christensen, C.H.; Nørskov, J.K. *Nano Today,* **2007**, *2*, 14.
12. Gasaymeh, S.S.; Radiman, S.; Heng, L.Y.; Saion, E.; Saeed, G.H.M. *Am. J. Appl. Sci.* **2010**, *7*, 892.
13. Biswal, J.; Misra, N.; Borde, L.; Sabharwal, S. *Radiat. Phys. Chem.* **2013**, *83*, 67.
14. Choi, S.; Lee, S.; Hwang, Y.; Lee, K.; Kang, H. *Radiat. Phys. Chem.* **2003**, *67*, 517.
15. Choi, S.; Park, H.G. *Appl. Surf. Sci.* **2005**, *243*, 76.
16. Ajitha, B.; Reddy, Y.A.K.; Reddy, P.S.; Jeon, H.J.; Ahn, C.W. *RSC Adv.* **2016**, *6*, 36171.
17. Lin, Y.; Qiao, Y.; Wang, Y.; Yan, Y.; Huang, J. *J. Mater. Chem.* **2012**, *22*, 18314.
18. Samim, M.; Kaushik, N.K.; Maitra, A. *Bull. Mater. Sci.* **2007**, *30*, 535.
19. Lee, H.; Kim, C.; Yang, S.; Han, J.W.; Kim, J. *Catal. Surv. Asia.* **2011**, 16, 14-27
20. Javaid, R.; Kawasaki, S.; Suzuki, A.; Suzuki, T.M. *Beilstein J. Org. Chem.* **2013**, *9*, 1156.
21. Javaid, R.; Kawanami, H.; Chatterjee, M.; Ishizaka, T.; Suzuki, A.; Suzuki, T.M. *Chem. Eng. J.* **2011**, *167*, 431.
22. Du, Y.; Chen, H.; Chen, R.; Xu, N. *Appl. Catal., A,* **2004**, *277*, 259.
23. Wu, S.; Yan, S.; Qi, W.; Huang, R.; Cui, J.; Su, R.; He, Z. *Nanoscale Res. Lett.* **2015**, *10*, 213.
24. Lin, C.; Tao, K.; Hua, D.; Ma, Z.; Zhou, S. *Molecules* **2013**, *18*, 12609.
25. Gangula, A.; Podila, R.; Ramakrishna, M.; Karanam, L.; Janardhana, C.; Rao, A.M. *Langmuir.* **2011**, *27*, 15268.
26. Patra, S.; Naik, A.N.; Pandey, A.K.; Sen, D.; Mazumdar, S.; Goswami, A. *Appl. Catal., A,* **2016**, *25*, 214.
27. McLaughlin, W.L.; Boyd, A.K.; Chadwick, K.N.; McDonald, J.C.; Miller, A. (Ed) Dosimetry for Radiation Processing, Taylor and Francis, London. **1980**.
28. Rao, Y.N.; Banerjee, D.; Datta, A.; Das, S.K.; Guin, R.; Saha, A. *Radiat. Phys. Chem.* **2010**, *79*, 1240.
29. El-Batal, A.I.; El-Baz, A.F.; Abo Mosalam. F.M.; Tayel, A.A. *J. Chem. Pharm. Res.* **2013**, *5*, 1.

30. Hanžić, N; Jurkin, T.; Maksimović, A.; Gotić, M. *Radiat. Phys. Chem.* **2015**, *106*, 77.
31. Mallick, K.; Wang, Z.L.; Pal, T. *J. Photochem. Photobiol., A,* **2001**, *140*, 75.
32. Abedini, A.; Daud, A.R.; Hamid, M.A.A.; Othman, N.K.; Saion, E. *Nanoscale Res Lett.* **2013**, *8*, 474.
33. Kumari, A.S.; Venkatesham, M.; Ayodhya, D.; Veerabhadram, G. *Appl. Nanosci.* **2015**, *5*, 315.
34. Tong, G.; Liu, T.; Zhu, S.; Zhu, B.; Yan, D.; Zhu, X.; Zhao, L. *J. Mater. Chem.* **2011**, *21*, 12369.
35. Lu, Y.; Mei, Y.; Drechsler, M.; Ballauff, M.; *Angew. Chem., Int. Ed.* **2006**, *45*, 813.
36. Venkatesham, M.; Ayodhya, D.; Madhusudhan, A.; Veera, B.N.; Veerabhadram, G. *Appl. Nanosci.* **2014**, *4*, 113.
37. Nalawade, P.; Mukherjee, T.; Kapoor, S. *Adv. Nanopart.* **2013**, *2*, 78.
38. Li, J.; Liu, C.Y.; Liu, Y. *J. Mater. Chem.* **2012**, *22*, 8426.
39. Lu, W.; Ning, R.; Qin, X.; Zhang, Y.; Chang, G.; Liu, S.; Luo, Y.; Sun, X. *J. Hazard. Mater.* **2011**, *197*, 320.
40. Bano, M.; Ahirwar, D.; Thomas, M.; Naikoo, G. A.; Sheikh M. U.; Khan, F. *New J. Chem.*, **2016**, *40*, 6787.
41. Jana, S.; Ghosh, S.; Nath, S.; Pande, S.; Praharaj, S.; Panigrahi, S.; Basu, S.; Endo T.; Pal, T. *Appl. Catal., A*, **2006**, *313*, 41.